Available online at www.sciencedirect.com
ScienceDirect
Applied Surface Science 253 (2007) 9506–9512
applied surface science
www.elsevier.com/locate/apsusc

Effect of incorporating nonlanthanoidal indium on optical properties of ferroelectric $Bi_4Ti_3O_{12}$ thin films

Caihong Jia [a], Yonghai Chen [b], Linghong Ding [a], Weifeng Zhang [a,*]

[a] School of Physics & Electronics, Henan University, Kaifeng 475004, PR China
[b] Key Laboratory of Semiconductor Materials, Institute of Semiconductors, Chinese Academy of Sciences, Beijing 100083, PR China

Received 9 February 2007; received in revised form 10 June 2007; accepted 11 June 2007
Available online 16 June 2007

Abstract

$Bi_4Ti_3O_{12}$ (BTO) and $Bi_{3.25}In_{0.75}Ti_3O_{12}$ (BTO:In) thin films were prepared on fused quartz and $LaNiO_3$/Si (LNO) substrates by chemical solution deposition (CSD). Their microstructures, ferroelectric and optical properties were investigated by X-ray diffraction, scanning electron microscope, ferroelectric tester and UV–visible–NIR spectrophotometer, respectively. The optical band-gaps of the films were found to be 3.64 and 3.45 eV for the BTO and BTO:In films, respectively. Optical constants (refractive indexes and extinction coefficients) were determined from the optical transmittance spectra using the envelope method. Following the single electronic oscillator model, the single oscillator energy E_0, the dispersion energy E_d, the average interband oscillator wavelength λ_0, the average oscillator strength S_0, the refractive index dispersion parameter (E_0/S_0), the chemical bonding quantity β, and the long wavelength refractive index n_∞ were obtained and analyzed. Both the refractive index and extinction coefficient of the BTO:In films are smaller than those of the BTO films. Furthermore, the refractive index dispersion parameter (E_0/S_0) increases and the chemical bonding quantity β decreases in the BTO and BTO:In films compared with those of bulk.

PACS : 77.84.Dy; 81.15.Fg; 78.55.Hx; 78.66.Li

Keywords: Ferroelectric thin film; Optical transmittance; $Bi_4Ti_3O_{12}$; $Bi_{3.25}In_{0.75}Ti_3O_{12}$; Chemical solution deposition

1. Introduction

Ferroelectric thin films have attracted much attention for the application in nonvolatile ferroelectric random memory (NvFRAM), microelectronic mechanical systems (MEMS), non-linear optical devices, surface acoustic wave devices, tunable capacitors, sensing applications or pyroelectric detectors [1]. The ever increasing demands for NvFRAM have lead to the search for a new material with a large spontaneous polarization and fatigue-resistant characteristics. Among various ferroelectrics, $Bi_4Ti_3O_{12}$ (BTO) is currently regarded as one of the most promising candidate materials for NvFRAM [2]. It is well known that bulk undoped BTO shows a very high remnant polarization ($2Pr = 100\ \mu C/cm^2$) [3], but thin films have much lower polarization [4]. To enhance the ferroelectricity such as increasing the remnant polarization of BTO, the substitution effect of lanthanoidal cations for Bi^{3+} has been studied ranging from small-sized Yb^{3+} to large-sized Ce^{3+} [5–8]. Recently, the substitution effect of nonlanthanoidal indium for Bi^{3+} on the ferroelectric properties was presented [9]. It was found that the remnant polarization values of the In-substituted BTO films were larger than those of the lanthanides substituted BTO films.

Meanwhile, doping indium in the opto-electronic oxides such as SnO_2 [10,11] and ZnO [12], has been reported to enhance the optical and electrical properties. On the other hand, most ferroelectric materials exhibit excellent optical properties. Thus, it is interesting to investigate the optical properties of indium doped BTO thin films, which has limited reports up to date. As the ionic radius of indium is more close to that of bismuth compared with other trivalent nonlanthanoidal elements, by doping indium in BTO, we expect to improve the transmittance in the visible and near-infrared region, and tailor the key parameters such as the single oscillator energy E_0, the average interband oscillator wavelength λ_0 and so on.

In this paper, undoped and indium doped bismuth titanate thin films are fabricated on quartz substrates by chemical

* Corresponding author. Fax: +86 378 3880 659.
E-mail address: wfzhang@henu.edu.cn (W. Zhang).

0169-4332/$ – see front matter © 2007 Published by Elsevier B.V.
doi:10.1016/j.apsusc.2007.06.013

solution deposition (CSD), and their topography, structures and optical properties are analyzed by scanning electron microscope (SEM), X-ray diffraction (XRD) and UV–vis–NIR spectrophotometer systematically, and the optical band-gap and the fundamental optical constants are derived.

2. Experimental

The resulting materials were bismuth nitrate pentahydrate [$Bi(NO_3)_3{\cdot}5H_2O$] (Wako Pure Chemical, 99.9%) and indium nitrate trihydrate [$In(NO_3)_3{\cdot}3H_2O$] (Wako Pure Chemical). According to the chemical composition of $Bi_4Ti_3O_{12}$ (BTO) and $Bi_{3.25}In_{0.75}Ti_3O_{12}$ (BTO:In), the required amount of bismuth nitrate and indium nitrate were added in glacial acetic acid (CH_3COOH) by stirring at 80 °C till they were completely dissolved. Stoichiometric titanium *n*-butoxide ($Ti(OC_4H_9)_4$) (analytical reagent, Kermel) was slowly dropped into the above solution under constant stirring. Appropriate amount of acetylacetone ($CH_3OCH_2COCH_3$) was used as stabilizer to inhibit probable precipitation in the solution. An 8% excess of bismuth nitrate was added to compensate for possible bismuth loss during high temperature treatment. The concentration of the final solutions was adjusted to 0.1 mol/L. The resultant solutions were stirred at room temperature for 2 h and filtered thereafter to form the stock solution, which were clear and transparent.

The precursor solutions were spin-coated on fused quartz or $LaNiO_3$/Si (LNO) substrates (4000 rpm, 20 s), then dried at 180 °C for 300 s, followed by pyrolyzed at 380 °C for 300 s, and finally annealed at 690 °C for 300 s in air. The heating rate during heat treatment is about 30 °C per second. A rapid thermal annealing process (RTP500) realized the crystallization of the BTO and BTO:In films. The multilayered thin films were deposited by repeating the procedures of spin-coating and heating treatment.

The crystalline structures and morphologies of the BTO and BTO:In thin films were determined by X-ray diffraction (XRD, DX2500), and field emission scanning electron microscope (FE-SEM, JEOL, JSM6300), respectively. The ferroelectric properties were measured for Au/BTO/LNO and Au/BTO:In/LNO capacitor structures by a ferroelectric test system (Precision Workstation, Radiant Technology). Circular Au top electrodes (7.065×10^{-4} cm^2) were fabricated by dc sputtering with a contact mask on the top of BTO and BTO:In thin films on LNO bottom electrodes. The optical transmittance of the BTO and BTO:In thin films on quartz substrates was recorded on a UV–vis–NIR spectrophotometer (Varian, Cary-5000) from 200 to 2500 nm. All measurements were carried out at room temperature.

3. Results and discussion

3.1. Microstructure characterizations

Fig. 1 shows the XRD patterns of BTO and BTO:In thin films on fused quartz and LNO substrates. For the thin films on fused quartz, the broadened peak at about 22° is from the quartz substrate, on which sharp peaks from the BTO and BTO:In films

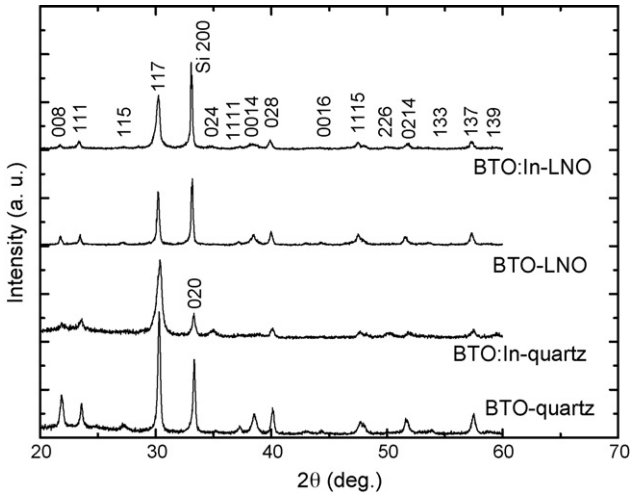

Fig. 1. XRD patterns of BTO and BTO:In thin films on quartz and $LaNiO_3$/Si substrates.

are overlapped. As can be seen, the films on both quartz and LNO substrates are polycrystalline with random orientation, and no obvious orientation change due to the substitution was observed. All the intense diffraction peaks could be indexed on the basis of the bismuth layered perovskite structure without the existence of a second phase [13]. It is observed that the XRD peaks in BTO:In films are wider than in case of BTO films, which indicates that the film is becoming slightly less crystalline with indium doping. The decrease in the crystallinity and grain size of BTO:In films may be understood from the fact that the incorporation of indium ions needs higher solution energies to form compensating point defects [14]. No obvious XRD spectra peak shifts were observed with indium doping. This is an indication that indium atoms substitute for bismuth atoms in BTO lattice without significantly affecting the lattice constant. The fact that indiums are smaller than bismuth ions (CN = 8, $r(In^{3+})$ = 0.92 Å, $r(Bi^{3+})$ = 1.17 Å) [15] makes this possible. Similar lattice behavior has been observed in the case of Y-doped BTO [16].

Fig. 2 shows the typical surface morphologies of the BTO and BTO:In films, depicted by SEM. It can be clearly seen that the grain size decreases with indium doping, which is correlated with the result of XRD. There is a strong tendency for the BTO particles to agglomerate. The cross-section observations on the BTO and BTO:In films show that no evident interdiffusion occurs between the quartz substrates and the films. The average thicknesses measured by SEM are about 0.60 and 0.62 μm for the BTO and BTO:In films.

From the atomic force microscopy (not shown here), it can be found that the root mean square (RMS) roughness of the BTO and BTO:In films are 30.79 and 16.11 nm, respectively. A considerable decrease in the surface roughness was observed in the BTO:In films, which may be owing to the reduction of grain size [17].

3.2. Ferroelectric measurements

Fig. 3 shows the hysteresis loops of the BTO and BTO:In thin films on LNO substrates measured at an applied voltage of

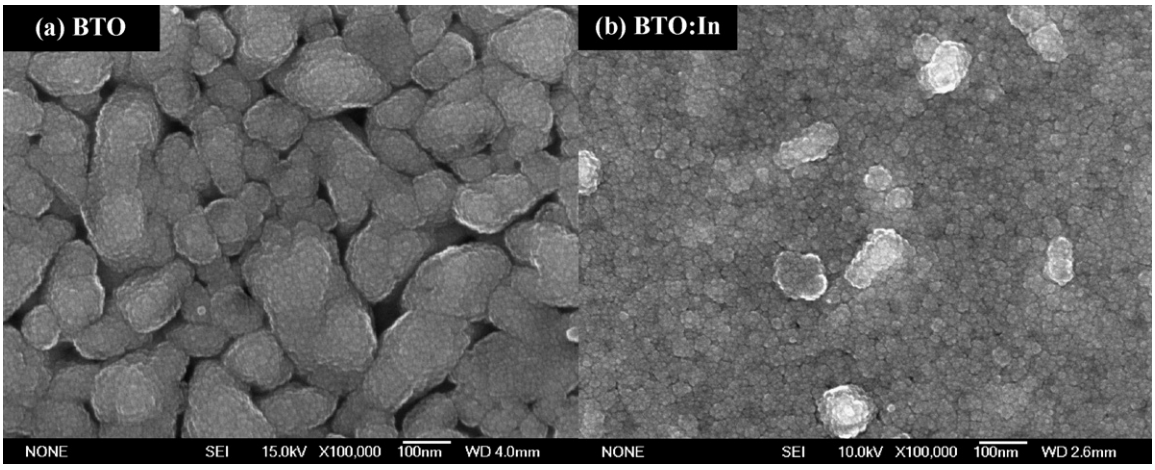

Fig. 2. SEM micrographs of BTO and BTO:In thin films on quartz substrates.

60 V. The hysteresis loops were measured in virtual ground mode. The remnant polarizations ($2P_r$) are 14.21 and 12.70 μC/cm^2, and the coercive voltages (V_c) are 22.54 and 18.31 V, respectively, for the BTO and BTO:In films. The remnant polarization and coercive voltage decrease a little with doping indium. The reduction of P_r and V_c observed in thin films may be ascribed to the reduction of grain size [18]. The reduction of V_c is useful to lower the applied voltage, while the reduction of P_r indicate weakening of the ferroelectricity of BTO. Chang and Bao [9] have investigated the ferroelectric properties of indium doped BTO thin films, and found that the P_r increases with doping indium. The difference about the increase and decrease of P_r may be owing to the difference of bottom electrodes used, as the bottom electrodes is essential to the ferroelectric properties [19].

3.3. Optical transmittance

The optical properties of BTO and BTO:In films on quartz substrates are investigated by optical transmittance measurements. Shown in Fig. 4 are the optical transmittance spectra. The oscillations in transmittance come from the interference due to reflection from the top surface of the film and the interface between the film and the substrate. The interference fringes and relatively high transmittance indicate a good homogeneity of the BTO and BTO:In films. The transmittance decreases drastically to zero at about 340 and 360 nm, and for light with a wavelength longer than 380 and 390 nm, the BTO and BTO:In films are transparent, respectively. From Fig. 4, it can be clearly seen that the transmittance increases with doping indium. As applications in opto-electronic devices based on optical waveguides require high transparent thin films, it is useful to minimize transmission loss.

The optical band-gap energies of the BTO and BTO:In films can be obtained from the transmittance spectra. The transmittance T varies exponentially with the absorption coefficient α near the absorption edge; therefore, α may be determined from the relation

$$T = A\exp(-\alpha d), \quad (1)$$

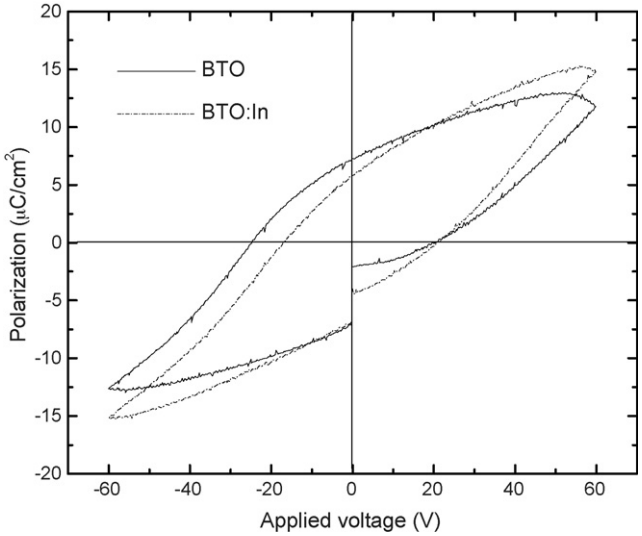

Fig. 3. Polarization-voltage hysteresis loops for the BTO and BTO:In films on $LaNiO_3$/Si substrates.

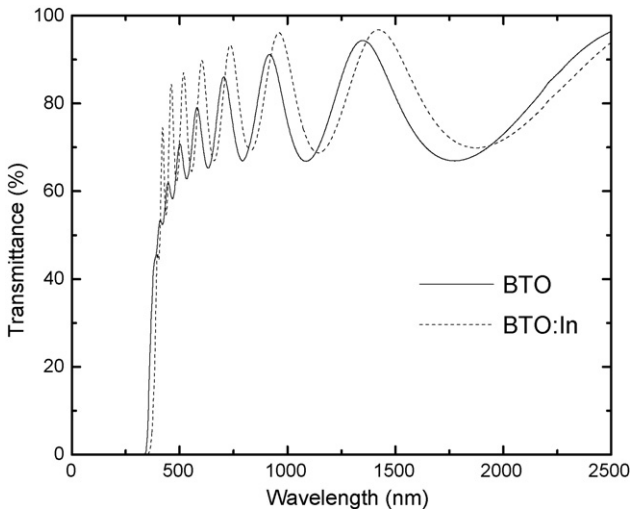

Fig. 4. Optical transmittance spectra of the BTO and BTO:In thin films on quartz substrates.

where d is the thickness of the film, and the parameter A is found to be nearly unity at the absorption edge. For a crystalline material, it was shown that the optical absorption near the band edge follows the equation [20]

$$(\alpha h\nu)^{2/n} = C(h\nu - E_g), \tag{2}$$

where α, ν, E_g, and C are absorption coefficient, light frequency, band-gap, and a constant, respectively. The parameter n decides the characteristics of the transition in a material. According to the Eq. (2), the values of n for the BTO and BTO:In films are determined to be 1 from the data in Fig. 4. This means that the optical transitions for the BTO and BTO:In films are both directly allowed. The E_g value can be estimated from the graph of $(\alpha h\nu)^2$ versus $h\nu$ by extrapolating the linear portion of the graph at higher energies to $(\alpha h\nu)^2 = 0$, shown in Fig. 5 [21]. It is shown that the introduction of indium reduced the E_g value from around 3.64 to 3.45 eV. Such a modification of band structure upon the indium substitution can be explained on the basis of the high electronegativity of the indium ion. It has been well known that the band structure of bismuth titanate (BTO) is generally defined by the Ti 3d level and O 2p level, which form conduction band (CB) and valence band (VB), respectively [22]. Considering the fact that the energy of electronic level of an element is inversely proportional to its electronegativity [23] and the substituted indium ion is more electronegative than titanium ion, the In 5s state is expected to have lower energy than the Ti 3d state, which leads to a lowering of CB and the narrowing of band-gap separation. Therefore, it becomes clear that indium ion can be a very powerful substituent for the band-gap engineering of bismuth titanate.

For weakly absorbing films on transparent quartz substrates, the linear refractive index and extinction coefficient as a function of wavelength can be obtained from the optical transmittance spectra using the envelope method proposed by Manifacier et al. [24]. It is a very useful and important approach to study the optical properties of oxide thin films, as most of the films satisfy the above weakly absorbing condition. Fig. 6 shows the relation between the refractive index and wavelength for the BTO and BTO:In thin films. As can be seen, the refractive index of BTO has a value of 2.28 in the near-infrared region and rises monotonically to 2.76 at 410 nm, while the refractive index of BTO:In gradually increases from 2.25 around 1423 nm to 2.66 at 421 nm. The refractive indices of both the BTO and BTO:In films are smaller than that that of the bulk single crystal [3]. Usually, the lower refractive index for films is supposed to be related to smaller packing density and defects. Since the films are not single crystals, but are composed of small crystallites, they are not as dense as the bulk material. So it is natural that the refractive indices of the thin films are lower.

It should be noted that the calculated refractive index of BTO:In films is smaller than that of BTO films. This is in accord with the phenomenon that the BTO:In films containing light ion (indium), as heavy ions such as Bi and Pb species usually possess larger index of refraction [25]. The difference in refraction index of the two materials provide a possible optical wave guide structure, in which BTO layer can serve as core materials and BTO:In layer can serve as cladding materials. Using the Lorentz–Lorenz model the packing density of the film, P, is given by

$$P = \left(\frac{n_f^2 - 1}{n_f^2 + 2}\right) / \left(\frac{n_b^2 - 1}{n_b^2 + 2}\right), \tag{3}$$

where n_f is the refractive index of the film and n_b is that of the single crystal [26]. Taking $n_b = 2.7$ (at 589 nm) for the BTO single crystal [3] and assuming that the value of n_b for BTO:In is the same with that of BTO single crystal, it can be derived that $P = 0.922$, and 0.903 for the BTO and BTO:In films, respectively. It can be seen that packing density values decrease with indium doping, which may be owing to the reduction of refractive index.

The average thicknesses of the BTO and BTO:In films, deduced from the transmittance spectroscopy, are 590 and

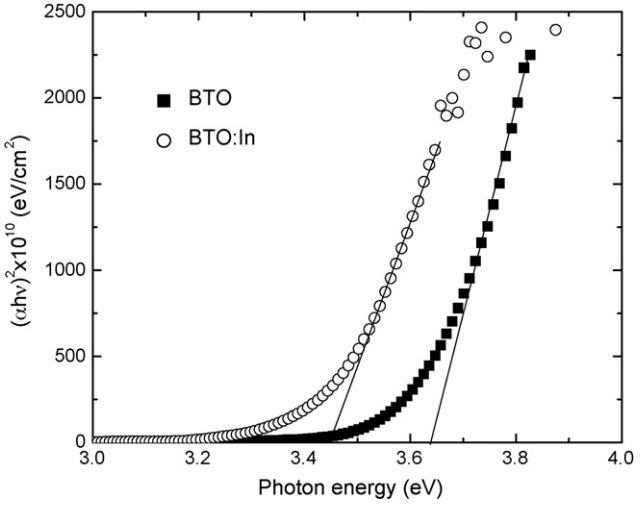

Fig. 5. Plot of $(\alpha h\nu)^2$ vs. $h\nu$ for BTO and BTO:In thin films on quartz substrates.

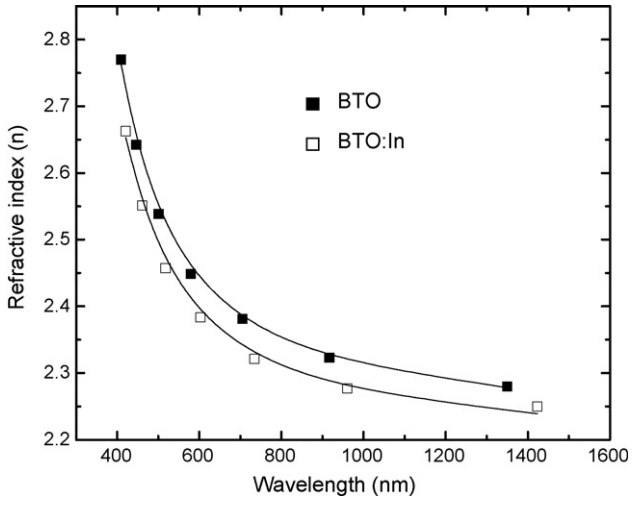

Fig. 6. Refractive index as a function of wavelength and the dispersion curve of BTO and BTO:In films on quartz substrates.

Table 1
Summary of the optical results for the BTO and BTO:In films on quartz substrates

Sample	Film thickness (nm) optical	Film thickness (nm) SEM	Refractive index, n (at 589 nm)	Extinction coefficient, k (at 589 nm)	Packing density (P)	Energy gap, E_g (eV)
BTO	590	600	2.46	0.04	0.922	3.64
BTO:In	630	620	2.40	0.01	0.903	3.45

Table 2
Dispersion parameters of the BTO and BTO:In films on quartz substrates

Sample	S_0 ($\times 10^{14}$ m^{-2})	λ_0 (μm)	E_0 (eV)	E_0/S_0 ($\times 10^{-14}$ eV m^{-2})	E_d (eV)	β (eV)	n_∞	ε_∞
BTO	0.62	0.2554	4.85	7.83	19.61	0.204	2.24	5.02
BTO:In	0.63	0.2493	4.97	7.89	19.46	0.202	2.22	4.93

630 nm, respectively. This result is consistent with those measured by SEM, indicating that the calculated parameters are reliable. Although the films were prepared using identical numbers of coating cycles, the thickness of the final annealed films varies. This occurred because the precursor solutions were not prepared at the exact same time, and there was a gradual rise in sol viscosity during storage (Table 1).

The dispersion data in the interband transition region are modeled under a single electronic oscillator. This theory assumes that the solid is composed of a series of the independent oscillators that are set into forced vibrations by incident light. Following the notation of Didomenico and Wemple [27], the refractive index is given by the well known Sellmeier dispersion relation:

$$n^2 = 1 + \frac{S_0\lambda_0^2}{1 - (\lambda_0/\lambda)^2}, \tag{4}$$

where λ_0 is an average oscillator wavelength position and S_0 is an average oscillator strength. The dispersion curve fits well to the experimental data, as shown in Fig. 6. A plot of $1/(n^2 - 1)$ versus $1/\lambda^2$ yields a straight line in Fig. 7. A linear relationship

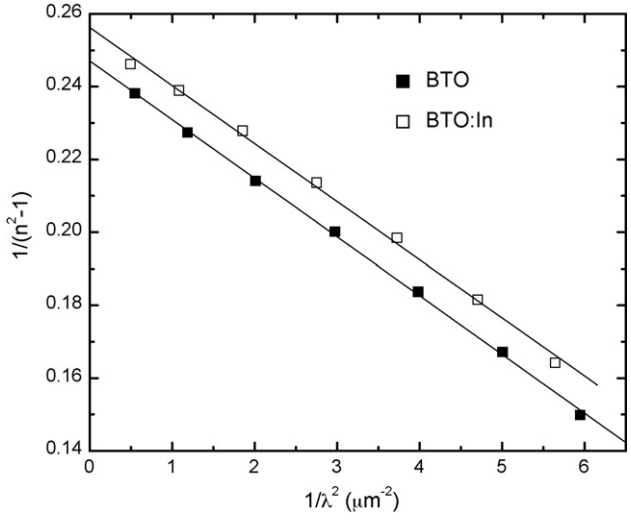

Fig. 7. Plot of $1/(n^2 - 1)$ vs. $1/\lambda^2$ for BTO and BTO:In films on quartz substrates.

confirmed the validity of the Sellmeier model in the visible and infrared region for BTO and BTO:In thin films. The parameters S_0 and λ_0 can be obtained from the slope ($1/S_0$) and the intercept ($1/(S_0\lambda_0^2)$) of the line. From the values of S_0 and λ_0, the energy of the oscillator E_0 (=hc/λ_0), where h is Plank's constant and c is the velocity of light) and the refractive index dispersion parameter (E_0/S_0) can be determined. The estimated dispersion parameters (S_0, λ_0, E_0, E_0/S_0) are presented in Table 2. The value of S_0 is nearly constant for both materials, as it is independent of the band-gap but depends strongly on the packing density relating with the preparation method [28]. However, the value of oscillator energy E_0 increases appreciably with doping indium, whereas the larger value of the refractive index dispersion parameter E_0/S_0 for the BTO:In films is due to the larger oscillator energy E_0. The quantity E_0/S_0, which depends upon various interband transitions, can be used to describe the optical dispersion behavior [27]. Didomenico and Wemple [27] reported that for a wide range of ferroelectric and non-ferroelectric materials the refractive index dispersion parameter (E_0/S_0) is constant at approximately $(6 \pm 0.5) \times 10^{-14}$ eV m^{-2}, which indicates that these very different materials exhibit a common refractive index dispersion behavior. The enhancement of refractive index dispersion parameter (E_0/S_0) in films compared with that of bulk has been also reported in literatures [29,30]. It is probably that nano-size grains in films leads to increased values in this parameter.

The obtained data of refractive index n can be also utilized to yield the long wavelength refractive index n_∞ using the following relation [31]

$$\frac{n_\infty^2 - 1}{n^2 - 1} = 1 - \left(\frac{\lambda_0}{\lambda}\right)^2 \tag{5}$$

where $n_\infty = (1 + S_0\lambda_0^2)^{1/2}$, the values of long wavelength dielectric constant $\varepsilon_\infty = n_\infty^2$ are shown in Table 2. Eq. (4) can also be expressed as [32,33]

$$n = \left(1 + \frac{E_0E_d}{E_0^2 - E^2}\right)^{1/2} \tag{6}$$

where E_d is the dispersion energy, $E_d = E_0S_0\lambda_0^2$. The dispersion energy E_d is a measure of the strength of the interband optical transitions, and can be considered as a parameter having very

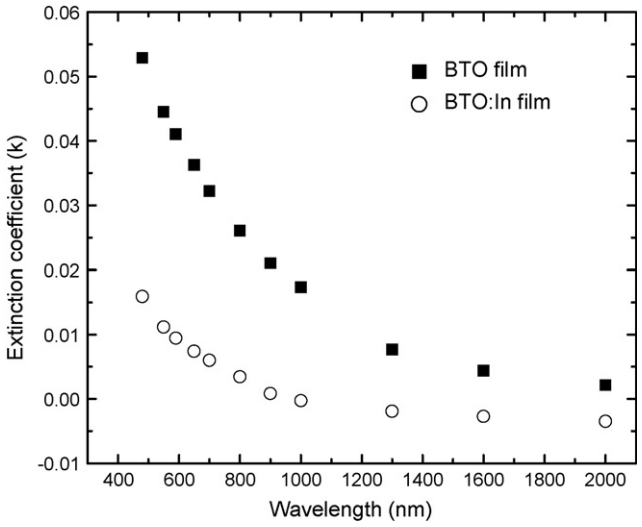

Fig. 8. Extinction coefficient k of BTO and BTO:In thin films as a function of wavelength on quartz substrates.

close relation with the charge distribution within unit cell and therefore with the chemical bonding. This chemical bonding quantity is given by

$$\beta = \frac{E_d}{N_c Z_a N_e} \quad (7)$$

where N_c is the coordination number of the nearest-neighbor cation, Z_a the formal anion valency, N_e the effective number of valence electrons per anions, and β is a quantity whose value depends on the chemical bonding character of material. $N_c = 6$, $N_e = 8$ and $Z_a = 2$ are estimated for BTO [32]. The chemical bonding quantity β has very nearly the same numerical value in large groups of crystals containing a single anion species. In particular, β is essentially two valued, taking on the ionic value, $\beta_i = 0.26 \pm 0.04$ eV, and taking on the covalent value, $\beta_c = 0.37 \pm 0.35$ eV. It is of interest that all the six-coordinated oxides have the ionic value of $\beta = \beta_i$, whereas the four-coordinated oxides seem to be either ionic or covalent, with ZnO falling at the ionic limit and ZnS at the covalent limit. It can be seen that the values of β for the BTO and BTO:In films are a little smaller than that of bulk. A similar reduction of β was also found in ZnO films [34]. It is probably that nano-size grains in films leads to reduction in the chemical bonding quantity β.

Fig. 8 shows the extinction coefficient k as a function of incident light wavelength. The extinction coefficients of BTO and BTO:In films are small at the longer wavelengths, where the BTO and BTO:In films are nearly transparent in the visible and near-infrared regions. It can be clearly seen that the extinction coefficient decreases with introducing indium, which is consistent with the transmittance enhancement shown in Fig. 4.

4. Conclusions

In summary, the BTO and BTO:In thin films were prepared on fused quartz and LNO substrates by chemical solution deposition process. The optical band-gap energy was found to be 3.64 and 3.45 eV for BTO and BTO:In films, respectively. The optical constants were determined from the transmittance spectra using the envelope method. The dispersion in the refractive index was fitted by the Sellmeier dispersion relation and described by a single electronic oscillator model. The packing densities for the BTO and BTO:In films calculated from the refractive indices are about 0.922 and 0.903, respectively. By contrast, the refractive index of the BTO:In film is smaller than that of the BTO film, which is owing to the fact that the indium species are lighter than the bismuth cations. The extinction coefficient of the BTO:In films is also found to be smaller than that of the BTO films, in accompany with the marked increase in transmittance. Furthermore, the refractive index dispersion parameter (E_0/S_0) increases and the chemical bonding quantity β decreases in the BTO and BTO:In films compared with those of bulk. It is probably that nano-size grains in thin films leads to variations in these parameters.

Acknowledgements

This work was supported by the Project of Cultivating Innovative Talents for Colleges and Universities of Henan Province and Open Research foundation of Henan University.

References

[1] J.F. Scott, Ferroelectric Memories, Springer, Berlin, 2000.
[2] Y.H. Wang, B. Gu, G.D. Xu, Y.Y. Zhu, Appl. Phys. Lett. 84 (2004) 1686.
[3] S.E. Cummins, L.E. Cross, J. Appl. Phys. 39 (1968) 2268.
[4] P.C. Joshi, S.B. Krupanidhi, Appl. Phys. Lett. 62 (1993) 1928.
[5] K.T. Kim, C.I. Kim, Mater. Sci. Eng. B 118 (2005) 229.
[6] H.C. Liu, B. Wang, R. Wang, X.R. Liu, Mater. Lett. 61 (2007) 2457.
[7] S.S. Kim, J.S. Song, S.C. Kwon, J. Crystal Growth 271 (2004) 90.
[8] C.H. Yang, Z. Wang, F.Y. Jiang, Y.L. Geng, B.Y. Zhu, X.Y. Yi, G.P. Ma, J.R. Han, J. Crystal Growth 271 (2004) 171.
[9] Y.C. Chang, D.H. Bao, Appl. Phys. Lett. 89 (2006) 072903.
[10] Z.G. Ji, Z.J. He, Y.L. Song, K. Liu, Z.Z. Ye, J. Crystal Growth 259 (2003) 282.
[11] Z.G. Ji, L.N. Zhao, Z.P. He, Q. Zhou, C. Chen, Mater. Lett. 60 (2006) 1387.
[12] C.S. Hong, H.H. Park, J. Moon, H.H. Park, Thin Solid Films 515 (2006) 957.
[13] JCPDS 65-2527.
[14] C.S. Liang, J.M. Wu, J. Crystal Growth 274 (2005) 173.
[15] R.D. Shannon, Acta Cryst. A32 (1976) 751.
[16] J. Ma, J. Gu, D. Su, X.M. Wu, C.H. Song, W. Li, X.M. Lu, J.S. Zhu, Thin Solid Films 492 (2005) 264.
[17] Z.B. Fang, Z.J. Yan, Y.S. Tan, X.Q. Liu, Y.Y. Wang, Appl. Surf. Sci. 241 (2005) 303.
[18] S. Chopra, S. Sharma, T.C. Goel, R.G. Mendiratta, Jpn. J. Appl. Phys. 43 (2004) 6193.
[19] A.Z. Simoes, A. Ries, F.M. Filho, C.S. Riccardi, J.A. Varela, E. Longo, Appl. Phys. Lett. 85 (2004) 5962.
[20] M.A. Butler, J. Appl. Phys. 48 (1977) 1914.
[21] J. Callaway, Quantum Theory of the solid state, Academic Press, New York, 1974, p. 525.
[22] J.W. Tang, Z.G. Zou, J.H. Ye, Chem. Mater. 16 (2004) 1644.
[23] S.G. Hur, T.W. Kim, S.J. Hwang, H. Park, W. Choi, S.J. Kim, J.H. Choy, J. Phys. Chem. B 109 (2005) 15001.
[24] J.C. Manifacier, J. Gasoit, J.P. Fillard, J. Phys. E: Sci. Instrum. 9 (1976) 1002.
[25] Y.M. Tsau, Y.C. Chen, H.F. Cheng, I.N. Lin, J. Eur. Ceram Soc. 21 (2001) 1561.

[26] T. Hubert, U. Beck, H. Kleinke, J. Non-Cryst. Solids 196 (1996) 150.
[27] M. Didomenico, S.H. Wemple, J. Appl. Phys. 40 (1969) 720.
[28] R. Thomas, D.C. Dube, Jpn. J. Appl. Phys. 39 (2000) 1771.
[29] Y. Du, M.S. Zhang, J. Wu, L. Kang, S. Kang, P. Wu, Z. Yin, Appl. Phys. A 76 (2003) 1105.
[30] S.B. Majumder, M. Jain, R.S. Katiya, Thin Solid Films 402 (2002) 90.
[31] T.S. Moss, Optical Properties of Semiconductors, Butterworth, London, 1959.
[32] S.H. Wemple, M. Didomenico, Phys. Rev. B 3 (1971) 1338.
[33] S.H. Wemple, M. Didomenico, Phys. Rev. Lett. 23 (1969) 1156.
[34] E.S. Tuzeman, H. Kavak, R. Esen, Phys. B. 390 (2007) 366.